# An investigation of Rubens flame tube resonances[a]

Michael D. Gardner[b] and Kent L. Gee
*Department of Physics and Astronomy, Brigham Young University, N283 Eyring Science Center, Provo, Utah 84602*

Gordon Dix
*JBL Professional, 8500 Balboa Boulevard, Northridge, California 91329*

The Rubens flame tube is a century-old teaching demonstration that allows observers to visualize acoustic standing wave behavior [H. Rubens and O. Krigar-Menzel, (1905). Ann. Phys. **17**, 149–164]. Flammable gas inside the tube flows through holes drilled along the top, and flames are then lit above. The tube is closed at one end and driven with a loudspeaker at the other end. When the tube is driven at one of its resonance frequencies, flames form a visual standing wave pattern as they vary in height according to the pressure amplitude in the tube. Although the basic performance of the tube has been explained [G. Ficken and C. Stephenson, (1979). Phys. Teach. **17**, 306–310], this paper discusses a previously unreported characteristic of the tube: a shift of the tube's resonance frequencies away from those predicted by simple introductory physics. Results from an equivalent circuit model of the tube and agreement between experiments and the model suggest that the shift is caused by the presence of the holes. For teachers and educators seeking to better understand and explain the tube to students, this article serves as a resource regarding the basic phenomena affecting the behavior of the tube. © *2009 Acoustical Society of America.* [DOI: 10.1121/1.3075608]

## I. INTRODUCTION

### A. History

In 1905, German physicists Rubens and Krigar-Menzel[1] discovered a way to demonstrate acoustic standing waves visually using what they referred to as a "flame tube." One hundred 2-mm diameter holes were drilled across the top of a round brass tube that was 4 m long and 8 cm in diameter. The tube was filled with coal gas and then flames were lit from the gas exiting through the holes on top. The tube was closed at both ends and driven at one of the ends with a tuning fork in a box. At resonances of the tube, the standing wave was seen in the flames above the tube with the flame height correlating with the pressure amplitude inside the tube.

### B. Classroom demonstration

Because the Rubens flame tube provides an exciting visual representation of sound waves, it naturally serves well as a teaching demonstration in the classroom setting of introductory physics or acoustics. When teaching about sound waves, it is common to talk about harmonically related resonances in pipes. The Rubens tube is suitable for a discussion of resonances because the resonances are easily seen: The flame height variation increases dramatically as resonance is reached. Because the tube was developed as a visual demonstration of a simple behavior, it has been used to foster student learning of basic physics principles. For example,

resonance-induced patterns in the flame have been used to explore basic relationships between frequency, wavelength, and sound speed. Via examples on the Internet, we are aware of students using the flame tube to deduce the speed of sound inside the pipe by measuring the distance between two peaks in the flame pattern and assuming that to correspond to a half-wavelength (e.g., see Fig. 1). With information regarding the wavelength and the driving frequency, a student then calculates the sound speed.

### C. Previous research

Although this demonstration is more than 100 years old, few studies have been published on the behavior of the Rubens flame tube. This is likely due to the fact that the tube is meant to demonstrate relatively simple physics; consequently, few have taken the time to study its behavior in detail. The most notable exception is Ficken and Stephenson,[2] who drove their flame tube with a directly coupled loudspeaker and showed that flame maxima occur at pressure nodes in the tube and flame minima at pressure antinodes. They explained this result using Bernoulli's equation, which indicates that the time-averaged mass flow rate of the gas is greatest at the pressure nodes. However, they showed that for low static gas pressures inside the tube or high acoustic amplitudes, the effect reverses, such that flame minima occur at the pressure nodes and the flame maxima occur at the pressure antinodes. This phenomenon has not been fully explained and may be the subject of future study.

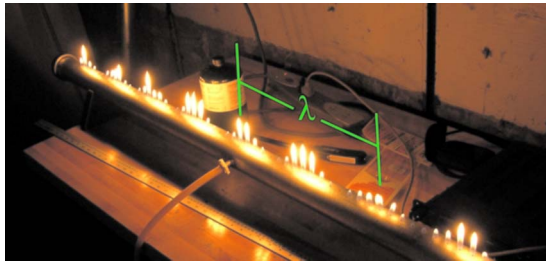In addition to the work of Ficken and Stephenson,[2] other short studies have been performed on aspects of the tube's

---

FIG. 1. (Color online) Hypothetical measurement of a wavelength in the tube using flame peaks produced by the standing wave pattern.



FIG. 2. T-network with source and termination ($Z_{AT}$).

behavior. For example, Jihui and Wang[3] discussed the relationship between flame height and pressure in the tube, while Spagna[4] researched the behavior of the flame itself. He tried to determine the phase relationship of the flame's flicker relative to the loudspeaker response, but found that his results were somewhat inconclusive. A direct extension of Rubens and Krigar-Menzel's work[1] is that of Daw,[5,6] who published articles detailing the construction and performance of square and circular flame tables that are used for visualizing two-dimensional modal patterns.

## D. Motivation

Although prior studies have addressed some aspects of the flame tube's performance, none of the investigations have discussed the relationship between tube resonance frequencies. Why might the neglect of this point be significant? Perhaps the answer is best illustrated by a direct example. During presentation of the seemingly simple physics of the tube in a department seminar at Brigham Young University, it was noted by one of the authors that the resonance frequencies of the flame tube used in the demonstration were not harmonically related as was expected from a simple explanation of the tube physics. Rather, the frequencies for the lower modes appeared to be shifted upwards and the cause for this shift was not obvious to him or to those in attendance. Anecdotally, in speaking with teachers at other institutions, we have discovered that others have observed similar phenomena in demonstrating the flame tube in their classes. Because the Rubens flame tube has been intended as a teaching tool to engage student interest in introductory classes, the shift in resonance frequency partially negates its effectiveness.

The results of the study presented in the remainder of this paper indicate that the modal frequency shift is due to the presence of the holes themselves, despite their small size relative to the dimensions of the tube. The holes create a Helmholtz-type resonance in the response of the tube that then causes the modal frequencies to be shifted upward. A Helmholtz resonator consists of a volume of gas in the bulk of a container acting as an acoustic compliance and a mass of air in the neck of the container acting as an acoustic mass. In the case of the flame tube, the volume of gas or acoustic compliance is the tube interior and the acoustic masses of air in each of the drilled holes create many Helmholtz resonators in parallel along the tube. These resonators notably affect the behavior of the tube as is shown through modeling and measuring tube behavior.
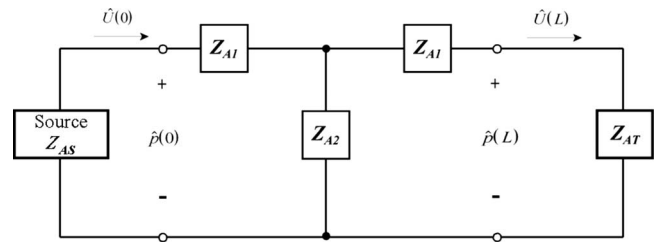
## II. METHODS

### A. Tube modeling

In order to better understand the tube and to quickly test parameter changes, an equivalent circuit model of the tube was developed as a direct adaptation of a similar model previously developed by Dix[7] for different purposes. Modeling of tubes with holes has been done before, notably by Plitnik and Strong[8] and Keefe,[9] in the application of musical instrument modeling. A summary of the equivalent circuit theory, based on Keefe's[9] development, used in modeling the tube follows.

For lumped-element systems (i.e., systems where all dimensions are small compared to wavelength), equivalent circuits can be used to calculate quantities such as volume velocity and pressure inside the tube as a function of frequency. In our case, we have chosen an impedance analog, where the acoustic pressure ($\hat{p}$) corresponds to voltage in the circuit, and the volume velocity ($\hat{U}$) corresponds to current. Because the tube's length is much greater than the cross-sectional dimensions and greater than some of the wavelengths of interest, a waveguide circuit is used to account for changing acoustic parameters along the longer dimension. Waveguide circuits translate impedances from a termination to an input location as[10]

$$Z_{AI} = \left( \frac{\rho_0 c}{S} \right) \frac{Z_{AT} + j(\rho_0 c/S)\tan(kL)}{\rho_0 c/S + jZ_{AT}\tan(kL)}, \tag{1}$$

where $Z_{AI}$ is the desired acoustic impedance at the input location, $c$ is the speed of sound, $S$ is the cross-sectional area of interest, $k$ is the wave number, $\rho_0$ is the fluid density, and $Z_{AT}$ is the acoustic termination impedance to be translated a distance $L$ down the tube. A waveguide circuit can also account for variable conditions along the length of the waveguide, or in our case, the presence of holes along the top.

In a waveguide circuit, two terms correspond to an arbitrary source and an arbitrary termination. The three other impedances make up the "T-network" in Fig. 2.

By equating the input impedance of this circuit to the impedance "translation" theorem in Eq. (1), one finds the series impedance terms $Z_{A1}$ (acoustic impedance) to be

$$Z_{A1} = j\left( \frac{\rho_0 c}{S} \right)\tan\left( \frac{kL}{2} \right) \tag{2}$$

and the shunt impedance term $Z_{A2}$ to be
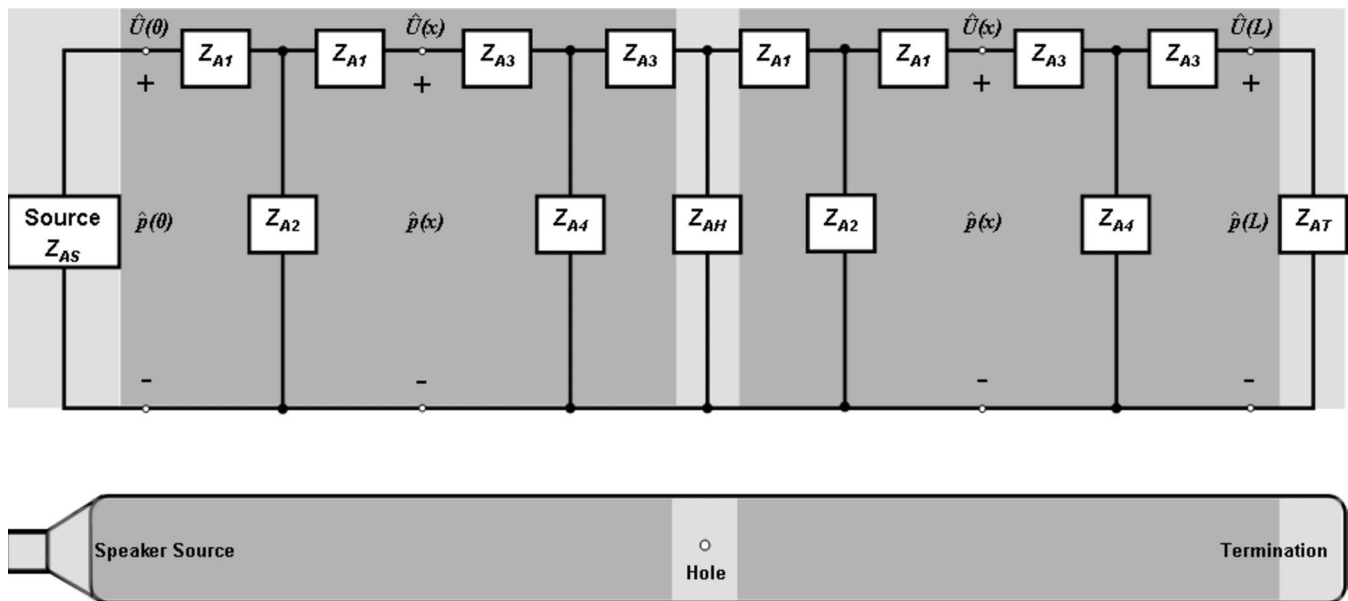
Gardner *et al.*: Rubens flame tube resonances

FIG. 3. Waveguide circuit diagram for a simple tube with source, termination, and one hole ($Z_{AH}$) with appropriate shading showing the impedance elements' corresponding physical objects.

$$Z_{A2} = -j\left(\frac{\rho_0 c}{S}\right)\csc(kL). \tag{3}$$

This circuit, comprised of Fig. 2 and Eqs. (2) and (3), describes pressure and volume velocity at the source and at the termination but not in between. Although the circuit serves as the foundation for the rest of the flame tube model, additions are needed to calculate the pressure along the length of the tube and to incorporate the presence of the holes.

To acquire acoustic quantities at points between the source and termination, a modification of the waveguide circuit is required. By coupling two T-network circuits together, the pressure or volume velocity can be obtained for any position $x$ by using the voltage (pressure) drop at the junction of the circuits. The impedances $Z_{A1}$ and $Z_{A2}$ remain the same, but now there are two more impedance quantities to solve for in the second T-network, namely,

$$Z_{A3} = j\left(\frac{\rho_0 c}{S}\right)\tan\left[\frac{k(L-x)}{2}\right] \tag{4}$$

and

$$Z_{A4} = -j\left(\frac{\rho_0 c}{S}\right)\csc[k(L-x)]. \tag{5}$$

By allowing $x$, which in this case represents the distance from the source end of the tube, to vary in Eqs. (4) and (5), the pressure or volume velocity may be calculated along the length of the tube.

To incorporate the holes at the top of the tube, only one major change is needed in the model. These holes represent a change in impedance that can be accounted for by taking multiple T-networks and juxtaposing them together with shunt terms for each of the holes. The sound pressure and volume velocity can then be modeled at the source, the termination, or any of the holes. To calculate the pressure or volume velocity at any point along the tube, two T-networks

are coupled together between each hole impedance, source, or termination impedance, schematically shown for one hole in Fig. 3. Note that in Eqs. (4) and (5) the definition of $x$ is changed to mean either the distance from the source or from the hole immediately to the left, whichever is closer.

The equivalent circuit theory is used to make a code that calculates the pressure along the length of the tube across a span of frequencies. The internal impedance of the source (the loudspeaker) is included and the volume velocity at the face is obtained using the Thiele–Small parameters. The cavity, a series of 2 cm gaps of varying diameter, is also included. The fluid properties are included as well, i.e., propane in the tube and air in the source cavity and loudspeaker enclosure. The frequencies at which the pressure amplitude is a local maximum at the termination (a rigid cap) are considered resonance frequencies. We numerically calculate the pressure at every point along the tube at all the frequencies of interest by multiplying the impedance and the volume velocity together as

$$\hat{p}(x) = \hat{U}(x)Z(x). \tag{6}$$

## B. Experiment setup

To study the impact of the holes on the shift in tube resonance frequencies and to compare against the equivalent circuit model, we constructed two flame tubes. The two galvanized-steel tubes are 1.524 m long with a 2.6 cm radius and have a 4 mm wall thickness. Both tubes have 60 deburred holes drilled in the top, each 2.2 cm apart, that begin 12 cm from the source end of the tube. The two tubes differ only in the size of the holes for the flames; one tube has 0.92 mm radius holes and the other has 0.46 mm radius holes, or half the size of the larger holes. Drilled in the center-side of each tube are 9.5 mm holes each with a short section of pipe used for the gas intake. A small hole was drilled in the
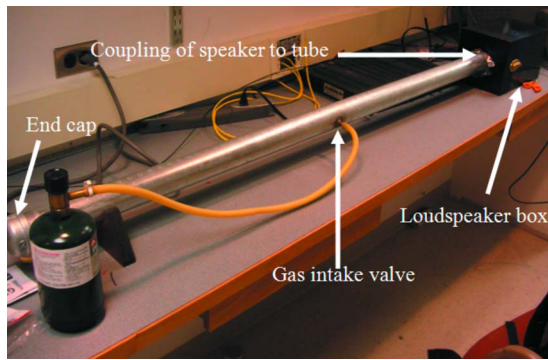
FIG. 4. (Color online) Flame tube setup.

| Parameter | Value | Units |
|-----------|-------|-------|
| $R_e$ | 5.42 | $\Omega$ |
| $L_1$ | 0.152 | mH |
| $L_2$ | 0.488 | mH |
| $R_2$ | 16.5 | $\Omega$ |
| $Q_{MS}$ | 3.03 | $\cdots$ |
| $C_{MS}$ | 482.8 | $\mu$m/N |
| $M_{MS}$ | 9.66 | g |
| $F_s$ | 73.7 | Hz |
| $Bl$ | 6.59 | Tm |

galvanized-steel end cap (termination) for the tube to accommodate the 6.35-mm (0.25-in.) GRAS Type 1 microphone used to monitor the acoustic pressures at the termination end of the tube. The entire flame tube setup is displayed in Fig. 4.

To drive the tube, an enclosed loudspeaker was coupled directly to the tube at the other end as shown in Fig. 5. A 10.5 cm diameter driver, whose measured Thiele–Small parameters are provided in Table I, was placed in a medium-density fiberboard enclosure sealed with putty. The driver radiates into the tube through a 2 cm deep cavity that is 15.3 cm in diameter. This 15.3 cm section is the largest cross-sectional dimension in the setup, which limits our one-dimensional circuit model to 1018 Hz in propane. Although not visible in Fig. 5, plastic wrap approximately 15 $\mu$m thick was inserted at the drive end of the tube to prevent propane from leaking into the loudspeaker enclosure from the tube. Figure 6 shows the large-holed flame tube operating, the mode with four pressure antinodes and three pressure nodes being clearly shown.

In order to compare the model and physical flame tube results, acoustical measurements are needed inside the tube. This is accomplished by inserting a microphone in the termination end of the tube. Because of the rigidity of the galvanized-steel end cap, pressure antinodes occur at this location at resonance. With white noise driving the loudspeaker, the frequency response is measured at the termination. This technique was used to measure the frequency response for both the small- and large-holed tubes with the

flames lit. These measured frequency responses become the benchmark for comparison between the modeled and measured tubes.

## III. RESULTS

### A. Equivalent circuit model

The first results to discuss are those of the modeled tube. In order to quickly change model parameters and easily visualize the results, a MATLAB®-based graphical user interface was developed. A user inputs into the model the relevant tube dimensions (tube radius, hole spacing, number, size, etc.), the speed of sound inside the tube, the density of the gas, and the relevant source model parameters. The model then outputs a graph of the magnitude of the pressure along the tube at whatever frequencies are chosen. Example results can be seen in Fig. 7 for the large-holed tube. The figure shows relative sound pressure level in the tube (white indicates greater level) as a function of frequency and position in the tube. Because propane is denser than air, we assume that the tube eventually completely fills with propane as the air is forced out through the holes. Based on the average of temperature measurements inside the tube during operation, the modeled propane was calculated to have a sound speed of 256 m/s and a density of 1.62 kg/m$^3$.

Figure 7 shows the sound pressure level variation inside the large-holed tube for a number of scenarios and it is worthwhile to discuss those in some detail. First, although Figs. 7(a) and 7(c) are for the tube modeled with a constant volume velocity source, rather than the loudspeaker, all results shown include the loudspeaker cavity for the sake of consistency. In Fig. 7(a), which neglects both the holes and the loudspeaker, the resonance frequencies (white lines) are harmonically related and have a high quality factor. Figure 7(b) extends the results in Fig. 7(a) by introducing the effects



FIG. 5. (Color online) Close-up of the coupling of the speaker to the tube with relevant dimensions.



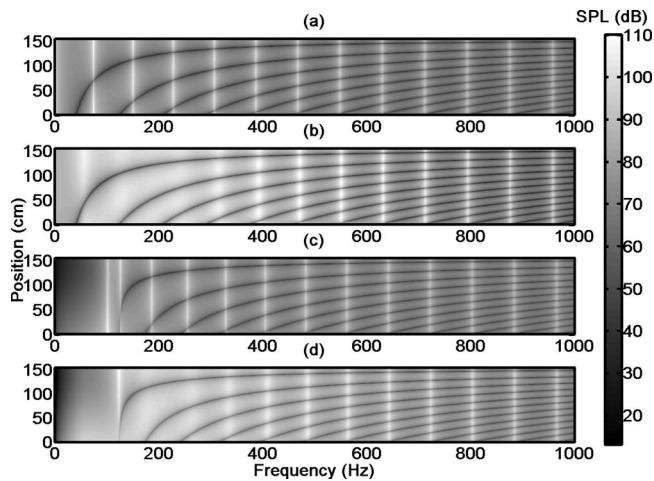FIG. 6. (Color online) Flame tube in operation.

FIG. 7. Graph of sound pressure level inside large-holed tube from the speaker end (0 cm) to the cap end (150 cm) looking at frequencies from 0 to 1000 Hz. (a) The graph is modeled *without* the source or holes but *with* the cavity. (b) *Without* the holes but *with* the source cavity and speaker. (c) *With* holes and cavity *without* the speaker. (d) *With* holes, cavity, and speaker.

of the speaker. The speaker alters the resonance frequencies and greatly decreases the quality factor of the lowest several modes. This is expected because the speaker has its own resonance at 73.7 Hz and introduces significant damping to the system. Figure 7(c) includes the effects of the holes with an ideal volume velocity source. Here, there are two effects to consider. First, we observe an additional resonance of the tube where the pressure level does not vary spatially. This is the Helmholtz resonance of the tube. Second, the natural frequencies of the first several modes are significantly shifted upward in frequency from the no-holed case in Fig. 7(a).

By including the loudspeaker and the holes in Fig. 7(d), the model comes closest to matching the actual experiment. Here, the presence of the coupled loudspeaker and the holes both reduces the quality factor of the lowest resonances and significantly shifts the frequencies of first several modes upward. It is clear from comparing Figs. 7(c) and 7(d) that the dominant cause of the overall resonance frequency shift above the first few low-quality-factor modes is due to the presence of the holes, not the loudspeaker. It is also worth noting that the interaction between the holes and the loudspeaker in Fig. 7(d) actually removes the Helmholtz mode from the response.

Before moving to the comparison of the modeled and physical flame tubes, a further illustration of the effect of the holes is worthwhile. To remove the effect of the real loudspeaker, we assume that our small- and large-holed tubes are driven with a constant volume velocity source (again, keeping the source cavity that is present in the physical tube). The resonance frequencies for the first nine modes are shown in Table II, along with the resonance frequencies for the tube without holes and the percent shift upward predicted. A comparison of the last two columns of Table II demonstrates that the resonance frequencies of the large-holed flame tube are significantly more affected by the holes than the small-holed tube. Using the large-holed tube as an example, examination of the spacing of the resonance frequencies themselves illustrates the possible difficulty encountered in trying to illustrate "simple physics" in a classroom setting. For the approximation that the tube is a simple closed-closed pipe, the resonance frequencies of the driven tube should be harmonically related. The average spacing of the resonance frequencies of the large-holed pipe is around 75 Hz, but the frequencies themselves are not multiples of 75 Hz and Fig. 7(c) reveals that there is no predicted resonance behavior below 100 Hz.

## B. Comparison of predicted and observed responses

The results in Table II were meant to examine the impact of the holes on the tube by themselves. The real system, however, will be impacted by the presence of the loudspeaker, as was modeled in Fig. 7(d). To compare the observed to the predicted modal frequencies, the frequency response magnitude at the termination position was plotted in decibels for both the model and as measured by the microphone at the end cap of the physical tube. The resonance frequency results for the large-holed tube with propane are displayed in Fig. 8. Again, the emphasis is on the frequencies, so the observed and predicted responses have been deliberately offset from each other. Although the agreement between the relative amplitudes for the first several modes is

TABLE II. Model-predicted resonance frequencies in propane for the three cases of the tube *with* the cavity: small holes, large holes, and no holes, including the percent shift from no holes. The tubes are driven by ideal constant volume velocity sources.

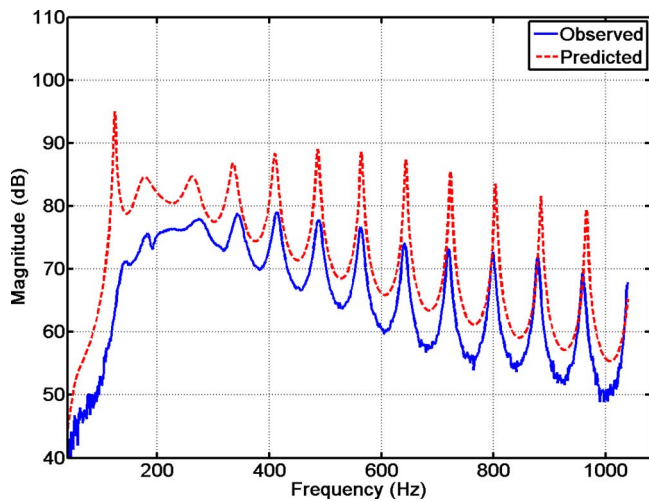| Mode No. | Small hole frequency (Hz) Helmholtz res. 60 Hz | Large hole frequency (Hz) Helmholtz res. 102 Hz | No hole frequency (Hz) | Small hole % shift | Large hole % shift |
|---|---|---|---|---|---|
| 1 | 92 | 127 | 75 | 22.7 | 69.3 |
| 2 | 162 | 187 | 151 | 7.28 | 23.8 |
| 3 | 236 | 255 | 228 | 3.51 | 11.8 |
| 4 | 314 | 329 | 307 | 2.28 | 7.17 |
| 5 | 392 | 405 | 387 | 1.29 | 4.65 |
| 6 | 472 | 483 | 467 | 1.07 | 3.43 |
| 7 | 552 | 562 | 548 | 0.73 | 2.55 |
| 8 | 643 | 641 | 630 | 0.48 | 1.75 |
| 9 | 726 | 722 | 711 | 0.42 | 1.55 |

FIG. 8. (Color online) Frequency response at the cap end of tube comparing the observed response (tube in operation) to the model predicted response in large-holed tube.
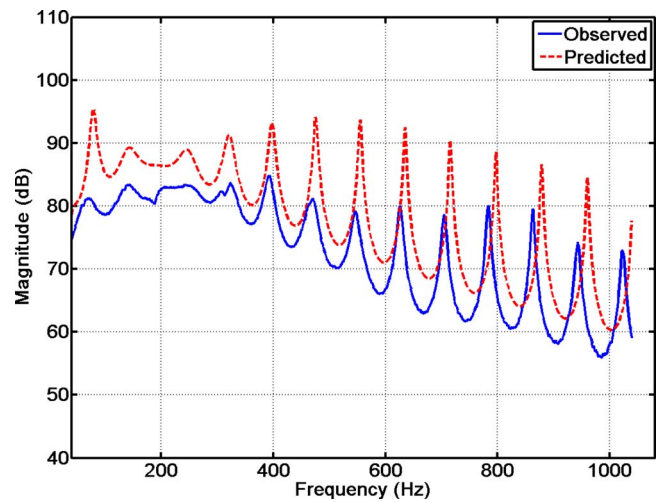


FIG. 9. (Color online) Frequency response at the cap end of tube comparing the observed response (tube in operation) to the model predicted response in small-holed tube.

not very well modeled, especially for the fundamental, the overall trend in the predicted and observed frequency shifts is readily observable. Similar results may be seen for the frequency response of the small-holed tube in Fig. 9. As with the large tube, there are some relative maxima and minima in the measured response that are absent from the predicted data below 300 Hz. Nevertheless, the measured and predicted responses both show the predicted upward shift in resonance frequency.

Table III quantifies the data in Figs. 8 and 9, showing both predicted and observed resonance frequencies for the small- and large-holed tubes. It also gives percentage error. The greatest error between predicted and measured frequencies is for the fundamental mode for both tubes. For the large-holed tube, the error is 17%, whereas for the small-holed tube, the error is 10%. Beyond the fundamental mode, the percentage error for all higher modes is less than 5% and is less than 2% in most cases. Hence, by including terms that account for the impedance of the holes and then calculating the resonance frequencies, the model accurately depicts the behavior of the tube and shows that the holes create the shift in resonance frequency. Based on altering various parameters within the model, we believe dominant source of error to be

uncertainty in our estimate of the sound speed in the tube. Although a constant sound speed was used in the model, the sound speed, proportional to the square root of temperature, varies within the actual tube because the tube is hotter in the middle (where the inlet is) and cooler on the ends.

## IV. DISCUSSION

Based on the results of the equivalent circuit model, it is clear that the holes are a primary cause of the shift in resonance frequencies. The fact that the lower modes are impacted more significantly than the higher modes can be qualitatively explained by considering the volume of gas in the hole as an acoustic mass, $M_A$, which is the actual mass of the gas divided by the square of the cross-sectional area of the hole. The acoustic impedance of the hole may then be written[11] as

$$\frac{\hat{p}}{\hat{U}} = j\omega M_A = j\omega M_M/S^2, \tag{7}$$

where $M_M$ is the (mechanical) mass of air inside the hole, including assumed flanged end corrections,[10] and $S$ is the cross-sectional area of the hole. Because the acoustic imped-

TABLE III. Predicted and observed resonance frequencies for both tubes and the error between the observed and the predicted. Note that there is no clearly observed distinction between the Helmholtz and the first mode.

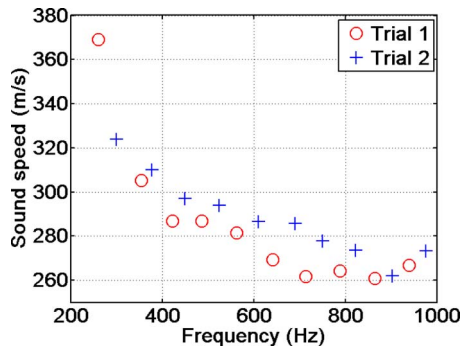| Mode No. | Small hole res. frequencies (Hz) | | Large hole res. frequencies (Hz) | | Small hole % error | Large hole % error |
|---|---|---|---|---|---|---|
| | Observed | Predicted | Observed | Predicted | | |
| 1 | 71 | 79 | 145 | 124 | 10 | 17 |
| 2 | 142 | 143 | 183 | 178 | 0.7 | 2.8 |
| 3 | 242 | 246 | 274 | 263 | 1.6 | 4.2 |
| 4 | 323 | 321 | 342 | 335 | 0.6 | 2.1 |
| 5 | 393 | 398 | 413 | 410 | 1.0 | 0.7 |
| 6 | 470 | 475 | 488 | 486 | 1.1 | 0.4 |
| 7 | 546 | 555 | 563 | 564 | 1.6 | 0.2 |
| 8 | 626 | 635 | 640 | 643 | 1.4 | 0.5 |
| 9 | 705 | 716 | 720 | 723 | 1.5 | 0.4 |

FIG. 10. (Color online) Calculated sound speed versus frequency using $c = \lambda f$ in large-holed tube. The distance between two flame peaks is used as a measurement of $\lambda$ and $f$ is the frequency input into the tube from the signal generator.

ance in the hole increases as a function of frequency, the holes play less of a role at high frequencies than at low frequencies and the tube begins to look like the no-hole case.

This same reasoning can be used to explain why the large-holed tube resonances are affected more than those of the small-holed tube. For a hole of constant length (the tube thickness in this case), $M_M$ increases linearly with volume and consequently, as a function of $S$. However, as shown in Eq. (7), as the diameter of the hole is made larger, the acoustic impedance is found to be inversely proportional to $S$. Therefore, the large-holed tube resonances are more affected than those of the small-holed tube because the greater cross-sectional area of the hole reduces $M_A$ and, therefore, the acoustic impedance of the hole. This may be useful information for one designing a tube: By making the holes as small as possible or the tube as thick as possible while maintaining sufficient mass flow rate of the flammable gas, the resonance frequency shift can be minimized.

It also must be noted that the loudspeaker affects the symmetry of the pressure response across the tube. The constant pressure resonance now decreases in amplitude away from the cap end, and symmetric modal responses are not expected. This occurs because the loudspeaker creates a boundary condition, which is dissimilar to that of a rigid cap: The tube is not "closed-closed." The loudspeaker's effect decreases with increasing frequency, because as its impedance increases as a function of frequency, it begins to act less like a compliant source and more like a closed end. In summary, we learn that the combined effect of the holes and loudspeaker shifts and smears the resonance frequencies, which are no longer harmonically related, and creates pressure asymmetry across the tube.

One implication of the results of this study is worth discussing. An example of how the wavelength of sound inside the flame tube could be measured via the flame pattern was shown in Fig. 1. Using this information and the drive frequency, one can use $c = \lambda f$ to calculate the sound speed inside the pipe. As a consequence of the shift in resonance frequencies due to the presence of the holes, this sound speed calculation practice will prove erroneous. Figure 10 shows the calculated sound speed based on measurements of the distance between flame maxima in the large-holed tube. For both trials, there is an apparent decrease in sound speed as a

function of frequency, which is physically untenable. The sound speed predicted by $c = \lambda f$, especially for the lower modes, is too high to be accurate, taking into account the gas inside the tube and its temperature. The sound speeds for the higher frequencies are closer to the actual sound speed, which we estimated to be about 256 m/s. Therefore, the flame peak distance is not a reliable source for the wavelength in the equation $c = \lambda f$. Information previously available on the Internet indicated that others have observed this apparently dispersive sound speed, but have not attributed it to the presence of the holes and the shift in resonance frequency. These results were confirmed using the equivalent circuit model, where one can readily observe that the distance between pressure maxima is greater than a half-wavelength. This results in an erroneous sound speed calculation for the lower modes. For the higher modes, however, the distance between adjacent pressure maxima approaches a half-wavelength, which again indicates that the holes play a decreasing role at higher frequencies.

## V. CONCLUSION

The Rubens flame tube serves well as a classroom demonstration, but calculating resonance frequencies or sound speeds is not a straightforward exercise of basic acoustics. Depending on how the tube is built, the phenomena observed here may or may not be strongly present. For example, smaller and fewer holes will decrease the resonance frequency shift and will allow an instructor to demonstrate and discuss the simpler physics in a quantitative fashion with greater accuracy. However, if the holes are too small or too far apart, this could compromise the effectiveness of the demonstration. In a more advanced setting, the tube could be used as a demonstration of parallel impedances or an example of acoustic masses, where it might be viewed as initially counterintuitive by students that the holes actually play less of a role at high frequencies where they look large relative to a wavelength. There are likely other uses for the flame tube, and instructors can take advantage of its complicated nature to teach students that the simple explanations of a physical system are often approximations that neglect potentially richer and important phenomena.

## ACKNOWLEDGMENTS

[1] H. Rubens and O. Krigar-Menzel, "Flammenröhre für akustishe beobach-tungen (Flame tube for acoustical observations)," Ann. Phys. **322**, 149–164 (1905).
[2] G. Ficken and C. Stephenson, "Rubens flame-tube demonstration," Phys. Teach. **17**, 306–310 (1979).
[3] D. Jihui and C. T. P. Wang, "Demonstration of longitudinal standing waves in a pipe revisited," Am. J. Phys. **53**, 1110–1112 (1985).
[4] G. Spagna, Jr., "Rubens flame tube demonstration: A closer look at the flames," Am. J. Phys. **51**, 848–850 (1983).
[5] H. Daw, "A two-dimensional flame table," Am. J. Phys. **55**, 733–737

(1987).

[6]H. Daw, "The normal mode structure on the two-dimensional flame table," Am. J. Phys. **56**, 913–915 (1988).

[7]G. R. Dix, "Development and comparison of highly directional loudspeakers," MS thesis, Department of Physics and Astronomy, Brigham Young University, Provo, UT, 2006.

[8]G. R. Plitnik and W. J. Strong, "Numerical method for calculating input impedances of the oboe," J. Acoust. Soc. Am. **65**, 816–825 (1979).

[9]D. H. Keefe, "Theory of the single woodwind tone hole," J. Acoust. Soc. Am. **72**, 676–687 (1982).

[10]L. E. Kinsler, A. R. Frey, A. B. Coppens, and J. V. Sanders, *Fundamentals of Acoustics* (Wiley, New York, 2000).

[11]L. L. Beranek, *Acoustics* (Acoustical Society of America, Woodbury, NY, 1996).

Gardner *et al.*: Rubens flame tube resonances